JOURNAL OF COMPUTATIONAL PHYSICS 79, 298–316 (1988)

Nonlinear Beam Plasma Interaction Using Finite Difference Methods

J. LAVERGNAT

CNET/CRPE, 3 Avenue de la République, 92130 Issy les Moulineaux, France

TH. LEHNER

Laboratoire de physique des milieux ionisés, École Polytechnique, 91128 Palaiseau, France

AND

A. Y. LE ROUX

UER Informatique et Mathématiques, Université de Bordeaux 1, 351 Cours de la Libération, 33405 Talence, France

Received April 16, 1985; revised November 9, 1987

We study the numerical solution of a hyperbolic system arising from the following physical problem: the interaction of a beam of particles and a plasma, both being described by a fluid model, which are coupled by the Poisson equation. The equations are solved by Lagrangian–Eulerian anti-diffusive techniques, combined with an antidiffused version of the Lax–Friedrichs scheme, in a one-dimensional semi-infinite system. This allows the use of Courant numbers well above one. An imposed boundary condition for the beam injection allows beam front and neutralisation effects to be described suitably. The main physical applicaton (as one is concerned with beam radiation) is the observaton of the saturation of the wave emission by trapping the beam in the wave it excites. © 1988 Academic Press, Inc.

1. INTRODUCTION

The present problem is a special case of the general beam/plasma interaction, this case being aimed to the study of the radiation (electromagnetic and electrostatic) of a density modulated beam injected in a plasma. The idea of a beam antenna in this context has been already put forward (see [1–3]). A natural antenna occurs, in the same sense, in the very low frequency range with ionospheric whistlers in space (see [4]). The use of a beam as an antenna could be a very powerful tool in active experiments in the ionosphere and magnetosphere in triggering wave–particle interactions. We restrict ourselves to a one-dimensional problem to try to

0021-9991/88 $3.00

investigate the nonlinear phenomena responsible for saturation of the waves emitted by the beam.

Of course, in a one-dimensional model, wave emission is merely electrostatic: only the unneutralized part of the beam can radiate. Mechanisms of saturation are numerous, however, even in this simple case: trapping of the beam particles in their own neutralization waves, or demodulation of the beam density, or even global beam velocity braking. We actually find the "classical" beam trapping effect as a saturation mechanism which is a priori by no mean obvious. A three-dimensional simulation would be excessively complex to undertake for the same purpose.

2. Linear Theory

We choose a fluid model for both plasma and beam particles. The main drawbacks of a fluid model should, however, be underlined at once: we neglect all velocity dispersion effects though they are important for wave emission, and wave discrimination will become problematical since the fluid electric field represents all the possible existing fields (wave field and unneutralized space charge field as well).

We are left with the following equations:
for the beam,

$$\frac{\partial n_b}{\partial t} + \frac{\partial}{\partial x}[n_b v_b] = 0, \tag{1}$$

$$\frac{\partial v_b}{\partial t} + \frac{\partial}{\partial x}\left[\frac{v_b^2}{2}\right] = \frac{\tau_b}{m_b} E, \tag{2}$$

for the electron plasma,

$$\frac{\partial n_e}{\partial t} + \frac{\partial}{\partial x}[n_e v_e] = 0, \tag{3}$$

$$\frac{\partial v_e}{\partial t} + \frac{\partial}{\partial x}\left[\frac{v_e^2}{2}\right] + \frac{1}{m_e n_e}\frac{\partial P_e}{\partial x} = \frac{\tau_e}{m_e} E, \tag{4}$$

with the Poisson equation,

$$\varepsilon_0 \frac{\partial E}{\partial x} = \tau_b n_b + \tau_i n_i + \tau_e n_e. \tag{5}$$

In these equations, n_b, n_e, and n_i are respectively the beam, electron, and ion plasma densities; v_b and v_e are the fluid velocities of the beam and of the electron plasma. The electric charges are denoted by τ_b, τ_e, and τ_i, and the masses by m_b

and m_e, respectively. The electric field is denoted by E, the electronic pressure by P_e and the vacuum dielectric constant by ε. We define the two constants

$$\alpha_b = \frac{\tau_b}{m_b}; \qquad \alpha_e = \frac{\tau_e}{m_e}.$$

Equations (1) and (3) are the density continuity equations. Equations (2) and (4) are the equations of motion. The ions will be taken as an immobile neutralizing background. Since $\tau_i = -\tau_e$, (5) may be rewritten as

$$\varepsilon_0 \frac{\partial E}{\partial x} = \tau_e(n_e - n_e^0) + \tau_b n_b, \tag{1.5}$$

where $n_e^0 = n_i = \text{constant}$.

Note that for an electron beam, τ_e and τ_b are both negative, n_e and n_b are always positive, but $n_e^0 - n_e$ can have either sign. The velocity v_b will be positive, and v_e can have locally either sign.

Equation (2), and also (4) when $P_e = 0$, are known as Burgers diffusionless equation (see [9]). They are coupled linearly by their right-hand side term with the Poisson equation and Eqs. (1) and (3). A conservation form may be given to (2) and (4) by introducing the momenta $q_b = n_b v_b$, $q_e = n_e v_e$.

We get the system

$$\frac{\partial n_b}{\partial t} + \frac{\partial q_b}{\partial x} = 0 \tag{1.1}$$

$$\frac{\partial q_b}{\partial t} + \frac{\partial}{\partial x}(q_b v_b) = \alpha_b n_b E \tag{1.2}$$

and

$$\frac{\partial n_e}{\partial t} + \frac{\partial q_e}{\partial x} = 0 \tag{1.3}$$

$$\frac{\partial q_e}{\partial t} + \frac{\partial}{\partial x}\left(\frac{q_e^2}{n_e} + \frac{P_e}{m_e}\right) = \alpha_e n_e E \tag{1.4}$$

with E given by (1.5) or (5).

This system is a basic set to be completed by a boundary condition for the beam injection at $x = 0$. The positive quantities $n_b(0, t)$ and $v_b(0, t)$ are given for all $t > 0$, in a "forced regime" of continuous injection. We also need to close the equations by an equation of state for P_e. The simplest one is the adiabatic approximation to be taken here as

$$P_e = V_{ad}^2 m_e n_e^\delta / \delta,$$

where

$$V_{ad}^2 = \delta k_B T_e/m_e = \delta V_{the}^2$$

with V_{the} denoting the thermal velocity, δ the adiabatic constant, k_B the Boltzmann constant, and T_e the electron temperature. For small perturbations we can linearize

$$P_e = V_{ad}^2 m_e n_e.$$

In the case of a nonconstant T_e, an additional heat equation should be written for it.

Introducing the Fourier Laplace transform one can examine the linear part of the basic set of equations.

For electrostatic perturbations, $\bar{E} = -\Phi_x$, Φ being the electrostatic potential, hence we are led to the equation with uniform beam, $n_b = \text{Cte}$:

$$k^2 \varepsilon_0 \bar{\Phi}(k, \omega)\, \varepsilon(k, \omega) = -\frac{\tau_b n_b v_b}{\omega(\omega - k v_b)} \tag{6}$$

and

$$\Phi(x, t) = -\frac{I_b}{\varepsilon_0} \int_L \frac{e^{i\omega t}}{\omega} \left[\int_{-\omega}^{+\infty} \frac{e^{-ikx}}{k\varepsilon(k, \omega)(\omega - k v_b)}\, dk \right] dt, \tag{7}$$

where $I_b = \tau_b n_b v_b$ is the beam current, and $\varepsilon(k, \omega)$ is the dielectric constant involving the well-known four normal modes and two plasma modes, one being a slow one, the other a quicker one. These modes are useful since they will trace the motion of waves on the characteristics used in the numerical session. We have

$$\varepsilon(k, \omega) = 1 - \frac{\omega_{pe}^2}{\omega^2 - k^2 V_{ad}^2} - \frac{\omega_{pb}^2}{(\omega - k v_b)^2}, \tag{8}$$

with

$$\omega_{pe}^2 = \frac{n_e^0 \tau_e^2}{m_e \varepsilon_0}, \qquad \omega_{pb}^2 = \frac{n_b \tau_b^2}{m_b \varepsilon_0}.$$

For a 100% density modulated beam, we have

$$n_b(x, t) = n_b^0 [1 + \sin(\Omega(t - x/v_b))] \tag{9}$$

with a modulation frequency Ω, and, instead of (6) (see [2]), we formally set

$$\varepsilon_0 k^2 \varepsilon'(k, \omega)\, \Phi(k, \omega) = \frac{i I_b}{\omega - k v_b} \left[\frac{\Omega}{\Omega - \omega} - \frac{1}{i\omega} \right],$$

where $\varepsilon' \neq \varepsilon$ is an unknown operator because of the strong density beam modulation. If it were known, the problem could be solved analytically.

For a modulated beam as given by (13), there is *no simple stability analysis* like the one yielding relation (8) but we expect suppression or control of the instability by the modulation (see [4]).

We can now introduce neutralization effects on the uniform beam model: neutralization means a reaction of the plasma which tends to cancel the charges τ (electric charge neutralization) and current I_b (current neutralization) brought in by the beam. If the neutralization were total, then only the front of the beam would be emissive and the level of radiated waves would be very weak. But as the beam is modulated, the plasma will not necessarily cancel the perturbations τ and I anywhere in x at any given time t, and we expect a nonzero wave electric field to be created. Actually, one has a secularly diverging field if one sticks to the previous linear analysis because of the degeneracy of the frequency poles $\Omega = \omega_{pe}$ in the Laplace inversion; this is not due to the instability. The field associated with neutralization (and emission) effects will be stationary in the beam reference frame and will appear at the Ω frequency as seen by the plasma electrons.

Note also the existence of a pole at $\omega = 0$ in (7), associated with the neutralization of the static beam space charge. There is a difficulty with energy conservation, the medium becoming inhomogeneous with the beam penetration. To ensure conservation one needs two time scales: a fast time scale associated with the high frequency wave at Ω, and a slow time scale associated with the static field at $\omega = 0$.

Here the net charge injected by the beam should be locally compensated by the plasma. One should also notice the two signs, from (8),

$$\frac{\omega}{k} = \pm V_{ad}$$

of the waves associated with plasma modes. This is important for the application of methods involving characteristics to be defined in the following section.

We conclude this section by emphasizing the originality of the present simulation using a semi-infinite model instead of methods based on the Vlasov or fluid equations written for cyclic boundary conditions with already prescribed injected particles that do not allow the description of front effects.

3. The Numerical Procedure

The velocity v_e is often close to the thermal velocity V_{ad} in practice, and both are far less than the beam velocity v_b: $v_b \gg v_e$; $v_b \gg V_{ad}$.

Thus the use of the same explicit scheme with a Courant–Friedrichs–Lewy (CFL) stability condition will give bad results for the thermal electrons advection. As a matter of fact, if the time increment Δt is imposed by the faster velocity v_b, it becomes too small for the slower one, and too small a Δt leads to a large amount of numerical diffusion. So we shall use two different mehods, suited for each velocity.

We take an explicit scheme with a CFL stability condition fo the electrons advection, and a combination of Lagrangian and Eulerian techniques for the beam. We call it a Lagrange–Euler technique. This last method allows a Δt which can be far larger than the one imposed by a CFL condition. Hence the time increment will be fixed by the scheme used to compute the slow electrons advection. In order to reduce diffusion effects, the CFL number will be choosen close to unity for this scheme. Moreover, an antidiffusion technique of the flux-corrected-transport (FCT) type will be performed at each step. Such methods are analysed in [6–9].

3.1. *Beam Advection*

This section is devoted to a Lagrangian technique adapted to the beam advection. It may be broken into three steps. The first one is a transport during a time step Δt, combined wih a projection (i.e., averaging) on a Lagrangian mesh. The second step involves a new projection from this mesh to a fixed Eulerian grid. Next, an antidiffusive FCT step is performed, with a correction which preserves stability properties. In this way the numerical diffusion, resulting mainly from the double projection, is reduced efficiently. Next, we introduce the term corresponding to the effect of the electric field during the same time Δt.

The computation of the beam advection is the same as approximating the equations

$$\frac{\partial}{\partial t} n_b + \frac{\partial}{\partial x}(n_b v_b) = 0, \tag{10}$$

$$\frac{\partial}{\partial t} v_b + \frac{\partial}{\partial x}\left(\frac{v_b^2}{2}\right) = 0. \tag{11}$$

for a time step Δt, since E will be introduced later. The second equation (11) is the well-known diffusionless Burgers equation, and we are looking for the weak solution satisfying the entropy condition (see [6]). As a matter of fact v_b may be discontinuous for nonincreasing initial data. Note that the monotone behavior may be lost by the effects of the electric field. The first equation (10) described the conservation of the density n_b which is transported by the velocity field v_b. The system (10), (11) is not strictly hyperbolic since it involves the double eigenvalue v_b. The beam density flux across a characteristic is zero from (10). However, two characteristics can meet one another along a curve of discontinuity of the beam velocity. Then a part of the beam density will be concentrated along shock trajectories. Thus, singularities of the Dirac type appear along these curves. This raises a new difficulty, which is to give a sense to the product of distributions $n_b v_b$, and to have a numerical scheme able to approximate such a product. We can get rid of it by introducing a function N such that $N_x = n_b$. Then N is a bounded increasing function and satisfies

$$\frac{\partial}{\partial t} N + v_b \frac{\partial}{\partial x} N = g(t), \tag{12}$$

where g is a known function depending on the boundary conditions. Namely,

$$g(t) = N(0, t)\, v_b(0, t) + \frac{\partial}{\partial t} N(0, t).$$

The values of N are easily computed along the characteristics, along shock trajectories by considering that the characteristics are fixed to the shock curve after they meet it. These values are obtained by solving the differential equation

$$\frac{d}{dt} N(x(t), t) = g(t),$$

along the characteristics of equation $x = x(t)$, with

$$\frac{dx}{dt}(t) = v_b(x(t), t).$$

The position at the time $t - \Delta t$ of a particle located at x at the time t is $x - \Delta t\, v_b(x, t)$. Then we get

$$N(x, t) = N(x - \Delta t\, v_b(x, t), t - \Delta t) + \int_{t-\Delta t}^{t} g(s)\, ds. \tag{13}$$

The formula (13) will be used in place of (10), since it allows one to give a meaning to N during a whole time step. Next we get n_b by computing the derivative N_x. A mass concentration on a shock trajectory corresponds to a jump of N.

Let h $(= \Delta x)$ be the space mesh size. We define the two families of cells for any integer i, $J_i = (ih, (i+1)h)$; $I_i = ((i-\frac{1}{2})h, (i+\frac{1}{2})h)$.

For the time discretization, we introduce an increasing sequence $\{t_n\}$, with $t_0 = 0$, and we define $r_n = (t_n - t_{n-1})/h$. The sequence $\{r_n\}$ is supposed to be bounded. For simplicity, the boundary data are constant on each time interval (t_{n-1}, t_n). The initial conditions are assumed to be constant on any cell J_i, for any integer $i \geqslant 0$.

We now construct a step of the Lagrange–Euler technique. Let $n \geqslant 1$; we suppose that the approximate solution $n_b^{n-1}(x, t_{n-1})$, $v_b^{n-1}(x, t_{n-1})$ are known for any $x \geqslant 0$, and a constant on any cell J_i, where the values are denoted by $n_{b,i}^{n-1}$ and $v_{b,i}^{n-1}$, respectively. We also set

$$n_{b,-1}^{n-1} = n_b(0, t_{n-1}), \qquad v_{b,-1}^{n-1} = v_b(0, t_{n-1}),$$

to take the boundary conditions into account. Then we build the sequence $\{x_i^n\}$, for $i \geqslant 0$, by

$$x_i^n = (i + \tfrac{1}{2})h + v_{b,i}^{n-1} r_n h. \tag{14}$$

This is an increasing sequence if, for any $i \geqslant 1$,

$$1 + 2r_n(v_{b,i+1}^{n-1} - v_{b,i}^{n-1}) \geqslant 0. \tag{15}$$

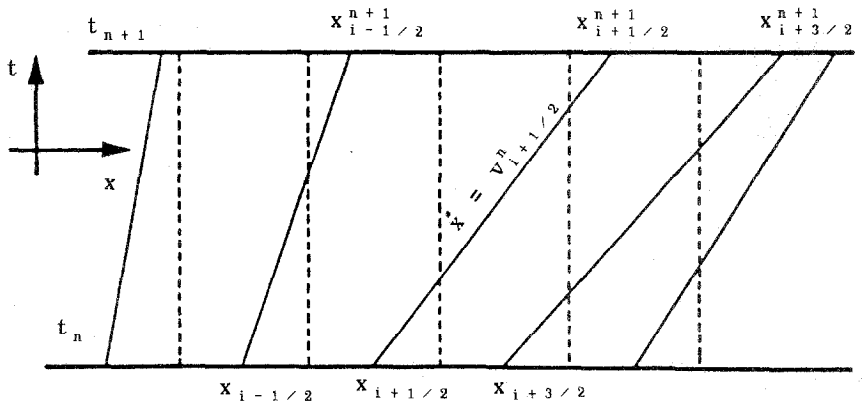

FIG. 1. The Lagrangian grid.

If $x_0^n > 0$, we set $x_{-1}^n = 0$. Condition (15) looks like a stability condition, which is never stringent in practice. Moreover, it is weaker than the CFL condition, and the scheme may be also extended to work without any condition. This is shown in Figs. 1 and 2, by performing a new numeration of the x_i^n when some cell collapses. Thus we have constructed the Lagrangian cells $I_i^n = (x_{i-1}^n, x_i^n)$.

Let v_b^n be the solution of (11) for $0 < x < \infty$ and $t_{n-1} < t < t_n$, computed from the starting values v_b^{n-1}, and the prescribed boundary data. We can compute its averaged value on each Lagrangian cell I_i^n. We get, for $i \geqslant 1$,

$$\tilde{v}_{b,i}^n = (v_{b,i}^{n-1} + v_{b,i+1}^{n-1})/2 \tag{16}$$

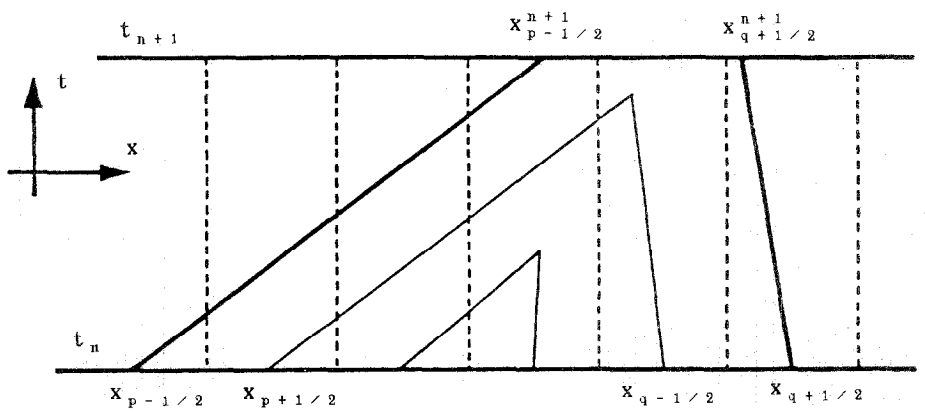

FIG. 2. Crossing of characteristics, to be jumped.

and for $i=0$,

$$(1+r_n h v_{\mathrm{b},0}^{n-1})\,\tilde{v}_{\mathrm{b},0}^{n} = (1+r_n h v_{\mathrm{b},0}^{n-1})\,v_{\mathrm{b},0}^{n-1} + r_n h (v_{\mathrm{b},-1}^{n-1})^2. \tag{17}$$

Now we compute

$$N_i^{n-1} = \frac{1}{2}\sum_{j=0}^{i} (n_{\mathrm{b},j-1}^{n-1} + n_{\mathrm{b},j}^{n-1})h$$

with $n_{\mathrm{b},-1}^{n-1}$ prescribed by the boundary data. From (13) we set, for $i \geqslant 0$,

$$N_i^n = N_i^{n-1} + g(t_{n-1})\,\Delta t$$

on I_i^n. We can now define a value for $\tilde{n}_{\mathrm{b},i}^n$, namely

$$(1+r_n h(v_{\mathrm{b},i}^{n-1} - v_{\mathrm{b},i-1}^{n-1}))\,\tilde{n}_{\mathrm{b},i}^n = \tfrac{1}{2}(n_{\mathrm{b},i}^{n-1} + n_{\mathrm{b},i-1}^{n-1}) \tag{18}$$

by differencing the N_i^n, for $i \geqslant 1$, and

$$(1+r_n h v_{\mathrm{b},0}^{n-1})\,\tilde{n}_{\mathrm{b},0}^n = n_{\mathrm{b},0}^{n-1} - 2r_n v_{\mathrm{b},-1}^{n-1} n_{\mathrm{b},-1}^{n-1} \tag{19}$$

for $i=0$. Then we have computed two functions, $\tilde{n}_{\mathrm{b}}^n$ and $\tilde{v}_{\mathrm{b}}^n$, defined on the Lagrangian mesh. They approximate n_{b} and v_{b} at $t=t_n$. Note that the introduction of N was very useful to define a scheme for the values of $n_{\mathrm{b},i}^n$; these values are directly computed from (18) and (19), in practice.

Next these two functions are averaged on the Euler mesh. This is very easy to perform and exactly computed since they are constant piecewise functions. The averaged values are denoted $n_{\mathrm{b},i}^n$ and $v_{\mathrm{b},i}^n$, respectively.

After these two steps, in order to get better results, an antidiffusion step is performed. It may be the following one, whose properties are analysed in [6]. We set

$$\begin{gathered} \Delta_i^n = (v_{\mathrm{b},i}^n - v_{\mathrm{b},i-1}^n)/2, \qquad s_{\mathrm{b}}^n = \operatorname{sign}(\Delta_i^n), \\ a_i^n = s_i^n \operatorname{Max}(0, \min(s_i^n \Delta_{i-1}^n, s_i^n \Delta_{i+1}^n, |\Delta_i^n|/2)), \\ \bar{v}_{\mathrm{b},i}^n = v_{\mathrm{b},i}^n - a_{i+1}^n + a_i^n. \end{gathered} \tag{20}$$

which gives the antidiffused values $\bar{v}_{\mathrm{b},i}^n$. The same process is adapted to the densities and builds the antidiffused values $\bar{n}_{\mathrm{b},i}^n$. Other techniques analogues to (20) may be found in [8]. Note that the two averages on J_i and the two antidiffusion steps are performed by the same subroutines, for the velocities and for the densities.

So far we have constructed the following scheme. First the Lagrangian mesh is computed by (14), under the condition (15). Then the averaged values $v_{\mathrm{b},i}^n$ and $n_{\mathrm{b},i}^n$ are computed by (16), (17) and (18), (19), respectively. Next a new averaging step, on the Euler mesh, is performed. This is followed by the antidiffusion step (20). In practice, the computation is performed on a finite interval $(0, R)$. Since v_{b} is never negative, no boundary condition is given at $x=R$.

3.2. *The Antidiffused Lax–Friedrichs Scheme*

For the advective part of the plasma equation (3), (4), it is possible to use the previous method, mainly for $P_e = 0$. But another solution can be used for a nonzero T_e: an explicit first order algorithm well suited for hyperbolic problems, stable under the classical CFL stability condition. This can be done by using the Godunov scheme, since Riemann solvers are easy to do, for a constant T_e. However, the well-known Lax–Friedrichs scheme gives ultimately better results provided that an antidiffused correction is performed. The one described in (20) can be used here also. The accuracy of this method is similar to the results obtained by the Godunov scheme. Moreover, this scheme, with the antidiffusion step, needs less CPU time and is far easier to program.

To fulfill the CFL condition is not very stringent, since both thermal and electron plasma velocities are far smaller than the beam velocity in practice. However, a difficulty appears in dealing properly with the boundary cells. Thus we shall use an antidiffused version of Lax–Friedrichs on any cell J_i, but on the boundary cells, a Godunov technique is employed.

We are concerned with the conservation laws (1.3), (1.4), where

$$P_e = [V_{ad}]^2 n_e m_e.$$

As in the previous section, we first study the homogeneous equation, i.e., when E is set to zero, for a time step. We use the same meshes as before. The algorithm also has three steps. By starting with approximate values of n_e and q_e constant on any cell J_i, we use the exact solution of (1.3), (1.4) from t_{n-1} to $t_{n-1} + r_n h/2$, and average it on any I_i. The second step is similar to the first one. By starting with these averaged values, the solution is computed from $t_{n-1} + r_n h/2$ to t_n and averaged one more time on the cells J_i. The third step involves antidiffusion as in (20) on n_e and q_e. We get, successively,

$$\bar{n}^n_{e,i} = (n^{n-1}_{e,i} + n^{n-1}_{e,i-1})/2 - r_n(q^{n-1}_{e,i} - q^{n-1}_{e,i-1})/2 \tag{21}$$

$$\bar{q}^n_{e,i} = (q^{n-1}_{e,i} + q^{n-1}_{e,i-1})/2 - r_n(F^{n-1}_i - F^{n-1}_{i-1})/2 \tag{22}$$

as the averaged values on I_i, with

$$F^{n-1}_i = (q^{n-1}_{e,i})^2/n^{n-1}_{e,i} + (V_{ad})^2 n^{n-1}_{e,i} \tag{23}$$

for the first step. The boundary cells will be considered later. Then we compute the averaged values on J_i,

$$\tilde{n}^n_{e,i} = (\bar{n}^n_{e,i} + \bar{n}^n_{e,i+1})/2 - r_n(\bar{q}^n_{e,i+1} - \bar{q}^n_{e,i})/2 \tag{24}$$

$$\tilde{q}^n_{e,i} = (\bar{q}^n_{e,i} + \bar{q}^n_{e,i+1})/2 - r_n(\bar{F}^n_{i+1} - \bar{F}^n_i)/2 \tag{25}$$

with $\bar{F}_i^n$ defined as in (23), for the second step. The last step consists in using the antidiffusion process described in (20) on the values

$$\tilde{n}_{e,i}^n \quad \text{and} \quad \tilde{q}_{e,i}^n$$

to get the values $n_{e,i}^n$ and $q_{e,i}^n$.

Handling the boundary conditions is more delicate, and we use the Godunov scheme in the boundary cells. In order to write this scheme, we have to solve the Riemann problem associated with (3), (4), with $E=0$. The Riemann invariants have the form

$$q_e = q_0 \pm V_{ad} n_e \log(n_e), \tag{26}$$

where q_0 is some constant; see Fig. 3. For an absorbing condition, we can set the inward Riemann invariant to a constant. This is the same as writing, at $x=0$,

$$q_e + V_{ad} n_e \log(n_e) = K_1 n_e \tag{27}$$

and at $x=R$,

$$q_e - V_{ad} n_e \log(n_e) = K_2 n_2 \tag{28}$$

for some given constants K_1 and K_2, and if

$$|q_e| \leqslant n_e V_{ad}. \tag{29}$$

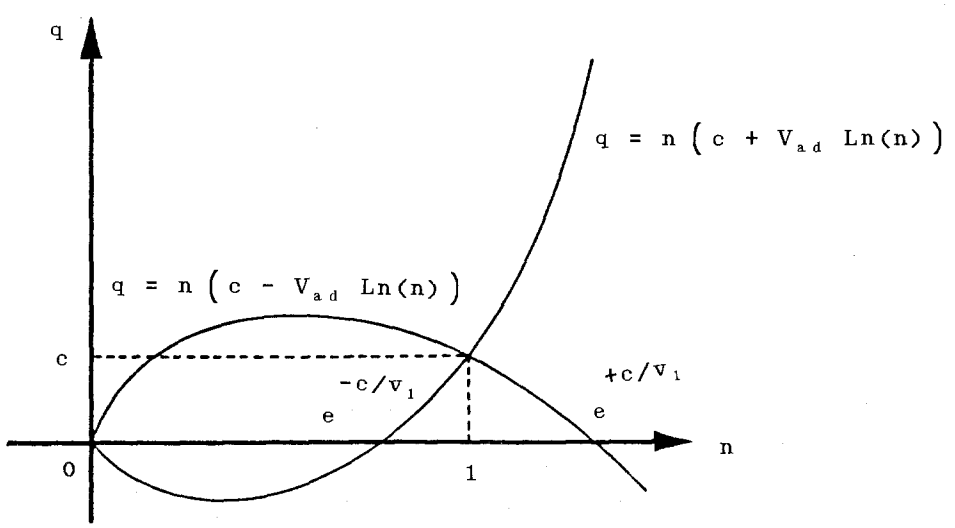

FIG. 3. Riemann invariant curves in the (q, n) plane.

The total length $R = Lh$ is taken large enough to avoid any perturbation of the physical phenomena under study.

For $|q_e| > n_e V_{ad}$, the two conditions (27) and (28) are to be prescribed at $x = 0$, and no condition is given at $x = R$. As a matter of fact, this never occurs in practice.

For reflexion conditions, we set $q_e = 0$ on the boundaries. Then a wave reaching the point $x = 0$ with a velocity $-V_{ad}$, reflects with the velocity $+V_{ad}$. We have the reverse at $x = R$.

Let us consider the bounded convex set

$$|q| + V_{ad} n \log(n) \leqslant K \tag{30}$$

for some constant K such that (30) is true for the initial and boundary conditions. Then the values of the approximate solution still belong to this bounded set after the two first steps (21), (22) and (24), (25). Thus nonlinear stability is ensured for this scheme.

3.3. *The Poisson Equation*

This equation can be integrated now. The forward boundary condition is given by causality, for there is no electric field ahead of the front of the beam. Thus we have

$$E(x, t_n) = 0$$

for $x \geqslant x'_n$, with x'_n such that

$$n_b(x'_n, t_n) = 0.$$

We get the values

$$\varepsilon_0 E_i^n = -\sum_{j=0}^{i} [\tau_b n_{b,j}^n + \tau_e n_{e,j}^n] h$$

and it remains to do

$$v_{b,i}^{n\,(\text{new})} = r_n h \tau_b E_i^n / m_b + v_{b,i}^{n\,(\text{old})}, \tag{31}$$

and

$$q_{e,i}^{n\,(\text{new})} = r_n h \tau_e E_i^n n_{e,i}^n + q_{e,i}^{n\,(\text{old})}. \tag{32}$$

from the values computed in Sections 3.1 and 3.2. More accurate methods, such as Gear techniques may be also used to introduce this term.

From a theoretical point of view, we have the following estimates. The densities n_b and n_e are positive and mass conservation holds. Thus E is still bounded. We deduce that the velocities v_b and v_e cannot increase faster than $\alpha_b t \operatorname{Max}(|E|)$. In the same way, $q_e = n_e v_e$ remains bounded, and by (30), the approximate solution (n_e, q_e) is valued in a bounded convex set, whose size is growing like

$K\alpha_0 t \operatorname{Max}(|E|)$, with $t>0$; see [8]. From these remarks, we get a linearly increasing estimate for the total energy W, with respect to the time t.

This energy W is defined as the sum

$$W = W_b + W_e + W_w,$$

with the beam kinetic energy

$$W_b = m_b n_b v_b^2/2,$$

the plasma kinetic energy

$$W_e = m_e n_e v_e^2/2,$$

and the fluid electrostatic field energy

$$W_w = \varepsilon_0 E^2/2.$$

We set

$$T = m_e V_{ad}^2 v_e \frac{\partial n_e}{\partial x},$$

by denoting the derivative of the adiabatic compressional energy with the plasma pressure P_e. Then we get the equation of energy conservation,

$$\frac{\partial W}{\partial t} + \frac{\partial}{\partial x}(W_b v_b + W_e v_e) + T = 0.$$

The numerical results and the previous estimates on the scheme have checked this conservation of energy. The preliminary tests also have shown the very good producibility of severely imposed discontinuities, such as shocks. This is mainly due to the use of antidiffusive phases. As a matter of fact, the use of a Lax–Friedrichs scheme without antidiffusion gives very damped results, which vanish rapidly; such experiments are reported in [10].

Indeed the Lagrangian technique in Section 3.1 corresponds to the projection of a particle method on a cell moving with the beam. The main merit of this projection consists in avoiding an expensive handling of the particle collisions, since the number of involved particles could be large. We mention that no pressure term arises in (11), which allows strong concentrations of particles at some points. Here we can get rid of the collapse of the Lagrangian cells and get an easier computation of the forthcoming interaction of the fast electrons with the slow ones, by performing one more projection on the fixed mesh. This projection induces exactly the same numerical diffusion as the Lax–Friedrichs scheme.

Now, since the same antidiffusion procedure can be used, we have chosen the Lax–Friedrichs scheme for computation of the slow electrons. The Lax–Friedrichs

scheme, with the antidiffusion procedure has been compared in [10] with the Godunov scheme with corrected flux (as in [9]). It has been checked that results of similar quality have been obtained with a much less CPU time for the Lax–Friedrichs scheme. Really the Godunov scheme reqires the use of a Riemann solver at the two edges of each cell, which is rather expensive.

4. Numerical Results

We write the normalized equations, and thus find the independent parameter of the system. These are the velocity ratio

$$b_1 = V_{ad}/v_b^0,$$

the density ratio

$$b_2 = n_b^0/n_e^0,$$

and the frequency detuning,

$$\delta_w = w_{pp} - \Omega.$$

In fact, for the classical beam plasma instability, $\delta_w = 0$, and the only scaling parameter is the O'Neil parameter (see [11–13]), S defined by

$$S = \left[\frac{b_2}{2b_1^2}\right]^{1/3} \quad \text{if } b_1 \neq 0, \qquad S = \left[\frac{b_2^2}{2}\right]^{1/3} \quad \text{if } b_1 = 0.$$

The grid parameters also have to be chosen: $\Delta x = h$, and $\Delta t = r_n h$. All lengths are normalized to the convective wave length, $\lambda = v_b^0 T$ at $t = 0$, and the time to the plasma period $T = 2\pi/w_{pp}$.

As a first test, we try a simulation without plasma, and for a uniform beam $n_b(0, t) = n_b^0$. Figure 4 shows the results of a typical run, where we have plotted the wave energy w_p which reduces to the beam potential energy into a vacuum as a function of time. We are thus able to check something like the energy equipartition principle (see the Appendix) in this case, since

$$|W_p| = 2W_F$$

at most. Here W_F is the beam kinetic energy injected at time t and used as a normalization factor on W_p.

We have

$$W_F = \tfrac{1}{2} m_b \int_0^t n_b(0, t)\, v_b(0, t)^3\, dt.$$

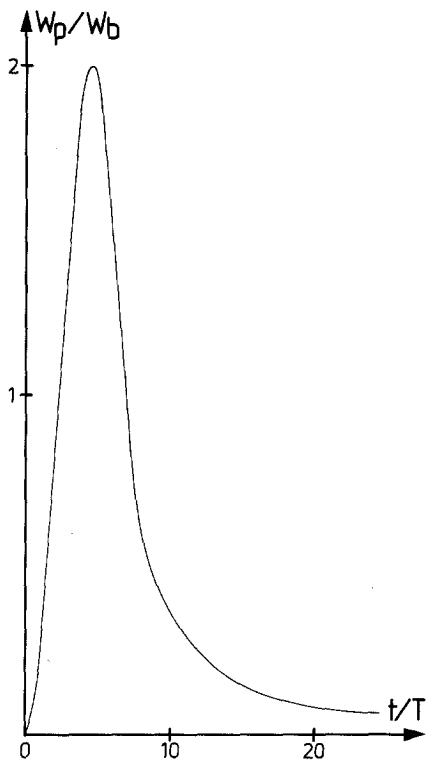

FIG. 4. Energy test on beam alone (no plasma). Beam potential energy W_p normalized to beam injected kinetic energy $W_b(t)$ versus time.

For the saturation value of W_p, all the beam is reflected by its own potential barrier, which remains unneutralized (apart from a weak "tunneling effect").

In the presence of a plasma, b_1 could not be chosen arbitrarily large. The flow can become quickly multivalued in velocities for too strong a b_1. Then the fluid equations no more hold, and a Vlasov equation is necessary to describe the velocity distribution. As a matter of fact, b_1 is less than 0.1 in practice, which justifies the arguments used for the choice of the numerical schemes.

Figures 5 to 7 show the result of a run without any electronic pressure. We set $T_e = 0$, then $b_1 = 0$, and $b_2 = 10^{-3}$, $h = \lambda/16$, $r_n = 0.5$; then $\Delta t = T/32$.

The left boundary conditions are

$$n_b(0, t) = n_b^0[1 + \sin(\Omega t/v_b^0)], \qquad v_b(0, t) = v_b^0$$

with $\Omega = w_{pp}$, thus $\delta_w = 0$.

No significant variation of data by detuning the frequency or by changing the initial phase in $n_b(0, t)$, has been found.

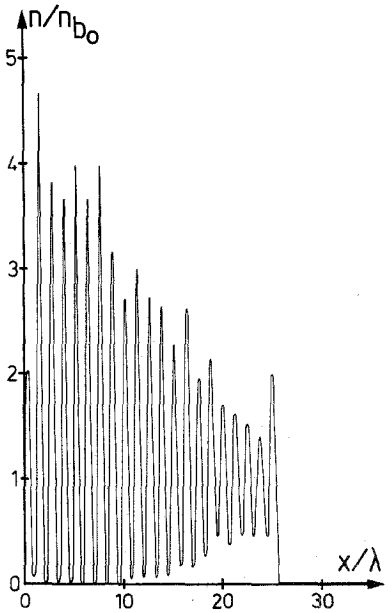

FIG. 5. Electric field versus space for a typical run (see text); $n = 1000$ time steps ($27.6\,T$), normalized to $E_0 = 1/(\varepsilon_0 \Omega)$.

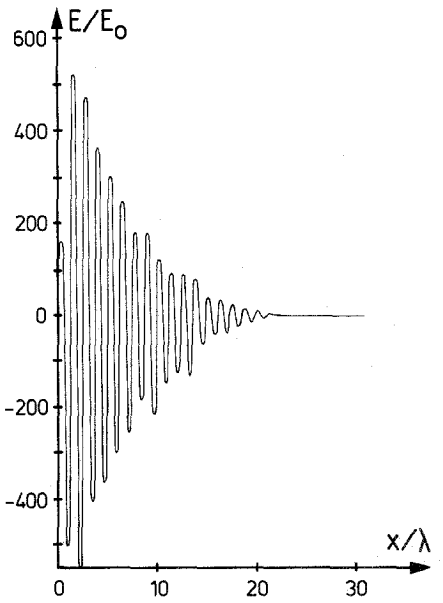

FIG. 6. Beam density versus space, $n = 1000$.

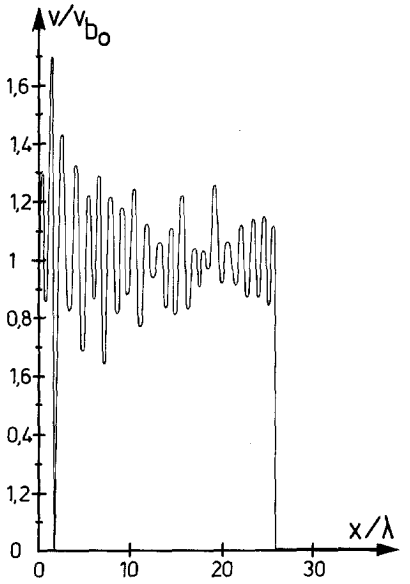

FIG. 7. Beam velocity versus space, $n = 1000$.

All results have been shown as functions of the spatial dimension $m\,\Delta x$, at time $t_n = n\,\Delta t$, with $n = 1000$. But, in fact, an instability has occurred in the Burgers equation at $n = 706$, and we have chosen to divide r by 2 to ensure stability again. The true time was near 27.6 plasma periods. Figure 5 shows the electric field normalized to the "coherent front" beam emission field (see [14]),

$$E_0 = \frac{1}{\varepsilon_0 \Omega}.$$

The quasi-symmetric oscillation at a constant frequency $\Omega = w_{pp}$ of E is obvious. The maximum E amplitude occurs at low x (near the injecton point) because of the space charge effects.

Figure 6 shows the beam density $n_b(x, t)/n_b^0$. Notice the good quality of the shock front; physically we can expect a demodulation or rather a keeping of the oscillating pattern of n_b between 0 and $2n_b^0$. But the regions of strong electric field lead possibly to "cavitation" like structures, where plasma density is expelled and can reinforce beam density causing n_b values larger than $2n_b^0$. Also discontinuities near the shock front could be responsible for these high values of n_b.

Figure 7 shows the fluid velocity normalized to v_b^0. It oscillates weakly in an anharmonic way and if one takes the average of the kinetic beam energy $n_b v_b^2$, we found that only a small fraction of it (typically less than 1%) could be transferred

to waves. But the velocity oscillates in such a way that it looks like trapping in the electrostatic field. Indeed, the trapping period is $T^* = 2\pi/\omega^*$, where

$$\omega^* = \left[\frac{|\tau_b| k |E(x, t)|}{m_b}\right]^{1/2}$$

is the bounce frequency, k being the local wave number. The $E^{-1/2}$ period dependence is roughly checked using Fig. 5, and a focusing effect of Figs. 5 and 7.

Of course, the trend of the formation of "vortex" like structure in the "*fluid*" space cannot lead to the usual trapping image and interpretation of plasma kinetic theory. Nevertheless, we can argue only here towards a trend to trapping, for if one takes a convective picture, $x' = v_b t$ gives $v(t)$ as an oscillating function able to execute closed orbits in "true" phase space (x, v).

We can conclude here that the beam emission level is governed by a mechanism of beam trapping in the developed electric field.

Appendix

It may be useful to split the energy into several parts, at least theoretically. The energy can be normalized to the total beam kinetic energy injected at time t, defined by $W_b(t)$, whereas the beam kinetic energy in the system is given by

$$W_b^1(t) = \frac{m_b}{2} \int_0^L n_b(x, t)\, v_b(x, t)^2\, dx,$$

which we expect is at most equal to $W_F(t)$. The total beam energy in the system is the sum of its kinetic and potential energies,

$$W = W_b^1 + W_p^1.$$

If we are in a vacuum with no external neutralization at all, we can easily compute W_b^1 from the Poisson equation

$$\varepsilon_0 E_x = \tau_b n_b (= \rho).$$

We get

$$E = -\frac{1}{4\pi\varepsilon_0} \frac{\partial}{\partial x} \int_0^L \frac{\rho(z, t)}{|x - y|}\, dz.$$

This allows us to get the equipartition of the energy

$$W_p^1 = \int_0^L \frac{\varepsilon_0}{2} E^2\, dx = \frac{1}{8\pi^2 \varepsilon_0} \int_0^L \rho(x, t) \left(\int_0^L \frac{\rho(z, t)}{|x - y|}\, dy \right) dx.$$

Here, we have used the expression for the energy density $\rho\Phi/2$, instead of $\varepsilon_0 E^2/2$, where Φ is the electric potential defined by $E = -\Phi_x$.

When the beam is injected into the plasma, the W_p^1 modulus is less than the value above, because of neutralization effects. It can be zero in case of perfect neutralization. It has an intermediate value in reality, difficult to predict other than numerically. Rough estimations could be done using the Debye screening effect, and considerations on the front of the beam can be done too; see [14].

So the global energy conservation is easy to test but it is difficult to have local details on the electric field in the fluid model because everywhere

$$\bar{E} = \bar{E}_{\text{neutr.}} + \bar{E}_{\text{wave}}$$

and we only know globally that the beam kinetic energy could be transferred to waves and he total electrostatic energy is built only by neutralization effects.

The problem finally amounts to making a correct energy conservation estimate in a material medium which has become inhomogeneous because of beam injection. Numerical experiments, from the properties of the scheme we have proposed, have shown good conservation of energy.

REFERENCES

1. J. LAVERGNAT AND R. PELLAT, in *Artificial Particle Beams in Space Plasma Studies*, edited by B. Crandall (Plenum, New York, 1982).
2. J. LAVERGNAT AND T. LEHNER, *IEEE Trans. Antennas* **AP-32**, 177 (1984).
3. J. LAVERGNAT, T. LEHNER, AND G. MATTHIEUSSENT, *Phys. Fluids* **27**, 1632 (1984).
4. J. DENAVIT, *J. Comput. Phys.* **15**, 449 (1974).
5. O. FUKUSAMA, Ph.D. thesis, University of Kyoto, Japan, 1981 (unpublished).
6. A. Y. LEROUX AND P. QUESSEVEUR, *SIAM J. Num. Anal.* **25**, No. 5, 985 (1984).
7. A. Y. LEROUX, *Math. Comput.* **37**, No. 156, 307 (1981).
8. A. Y. LEROUX, in *Computing Methods in Applied Sciences and Engineering V, 1981*, edited by R. Glowinski and J. L. Lions (North-Holland, Amsterdam, 1982), p. 347.
9. D. L. BROOK, J. P. BORIS, AND K. H. HAIN, *J. Comput. Phys.* **18**, 242 (1975).
10. B. BEN BARKA, E. LE GRUYER, A. Y. LEROUX, AND P. QUESSEVEUR, Rapport de contrat C. E. Gramat, 1983 (unpublished).
11. T. O'NEIL, *Phys. fluids* **8**, 2255 (1965).
12. T. O'NEIL AND J. H. WINFREY, *Phys. Fluids* **14**, 2796 (1971).
13. T. O'NEIL AND J. H. WINFREY, *Phys. Fluids* **15**, 1514 (1972).
14. J. LAVERGNAT AND R. PELLAT, *J. Geophys. Res.* **84**, 242 (1975).